Acta Pharmacologica Sinica (2010) 31: 616–628
 1671-4083/10 $32.00
www.nature.com/aps

Original Article

Transcriptional response of *Candida albicans* biofilms following exposure to 2-amino-nonyl-6-methoxyl-tetralin muriate

Rong-mei LIANG[1, 2], Yong-bing CAO[1, *], You-jun ZHOU[3], Yi XU[1], Ping-hui GAO[1], Bao-di DAI[1], Feng YANG[4], Hui TANG[3], Yuan-ying JIANG[1, *]

[1]Department of Pharmacology, School of Pharmacy, Second Military Medical University, Shanghai 200433, China; [2]Department of Pharmacy, General Hospital of Chengdu Military Command Region, Chengdu 610083, China; [3]Department of Medicinal Chemistry, School of Pharmacy, Second Military Medical University, Shanghai 200433, China; [4]Department of Pharmacology, School of Pharmacy, China Pharmaceutical University, Nanjing 210009, China

Aim: To identify changes in the gene expression profile of *Candida albicans* (*C albicans*) biofilms following exposed to 2-amino-nonyl-6-methoxyl-tetralin muriate(10b) and clarify the mechanism of 10b against *C albicans* biofilms.
Methods: Anti-biofilm activity of 10b was assessed by tetrazolium (XTT) reduction assay and the action mechanism against biofilms was investigated by cDNA microarray analysis and real-time RT-PCR assay.
Results: Ten differentially expressed genes were directly linked to biofilm formation and filamentous or hyphal growth (*eg*, *NRG1*, *ECE1* and *CSA1*). Decreased gene expression was involved in glycolysis (*eg*, *HXK2* and *PFK1*) and antioxidant defense (*eg*, *SOD5*), while increased gene expression was associated with enzymes that specifically hydrolyzed β-1,3 glucan (*XOG1*), and with lipid, fatty acid and sterol metabolism (*eg*, *SLD1*, *ERG6* and *ERG2*). Functional analysis indicated that addition of anti-oxidant ascorbic acid reduced inhibitory efficiency of 10b on mature biofilm.
Conclusion: Inhibition of 10b on biofilm formation possibly depends on impairing the ability of *C albicans* to change its morphology via altering the expression of biofilm formation genes. Mitochondrial aerobic respiration shift and endogenous ROS augmentation might be a major contribution to reduce mature biofilm metabolic activity. The data may be useful for the development of new strategies to reduce the incidence of device-associated infections.

Keywords: 2-amino-nonyl-6-methoxyl-tetralin muriate; anti-biofilm activity; action mechanism; microarray analysis; *Candida albicans*

Acta Pharmacologica Sinica (2010) 31: 616–628; doi: 10.1038/aps.2010.33; published online 12 April 2010

Introduction

C albicans is a dimorphic species capable of changing its morphology from the yeast form to the hyphal form, an all-important process to form mature biofilms and a transition critical to its pathogenesis[1–3]. Biofilm structure impairs the action of phagocytic cells from the immune system and antimicrobial agents[4–6], which are notoriously difficult to eradicate as well as an important source of many recalcitrant infections.

Biofilm development occurs in three phases over a period of 24–48 h[7–9]. The initial phase begins with adherence of single cells to the substratum. Second, attached cells proliferate to form microcolonies and begin to deposit an extracellular matrix. Finally, once cells reach confluency, the network of yeast cells transits to filamentous (pseudohyphal and hyphal) forms, which become encased in the exopolymeric matrix. Baillie and Douglas[10, 11] reported that slow growth of microorganisms, presumably due to some form of nutrient limitation, may contribute to mature biofilm resistance.

Beta-1,3 glucan is thought to be the main component of the three-dimensional matrix surrounding biofilm cells and closely tied to biofilm formation[12]. Nett *et al*[13] showed that elevated beta-1,3 glucan levels were characteristic of biofilm cells as compared to planktonic free-living *C albicans* cells. A complex network of signaling pathways regulates yeast-hyphal morphogenesis. It is known that several signaling pathways, including Cph1-mediated mitogen-activated protein kinase and Efg1-mediated cyclic AMP/protein kinase A, participate in the regulation of morphological transition[14, 15]. These multiple pathways in conjunction with the pathway-

* To whom correspondence should be addressed.
E-mail ybcao@vip.sina.com (Yong-bing CAO)
jiangyysmmu@163.com (Yuan-ying JIANG)
Received 2009-12-24 Accepted 2010-02-24

specific transcription factors regulate the expression of hypha-specific genes, including *ECE1, HWP1, HYR1, ALS1, ALS3, RBT1, RBT4,* and *HGC1*[16–21]. Hyphal development is negatively regulated by transcriptional repressors Tup1, Nrg1, Sfl1, and Rfg1[22–25]. Sfl1 has a dual function in filamentous growth of *C albicans*: it acts as a repressor of hyphal development antagonizing activation of Flo8 but functions as an activator releasing from inhibition of Flo8 in the matrix at low temperature. Rfg1 is a second DNA-binding protein that targets Tup1 to promoters of hypha-specific genes. Tup1 functions with DNA binding proteins Nrg1 and Rfg1 as a transcription regulator to repress the expression of hypha-specific genes. Nrg1 is a zinc finger DNA-binding protein that represses hypha-specific genes in a Tup1-dependent manner, making a major contribution to the repression of hyphal development[26].

Biomaterial infections are an increasingly alarming problem. Given their intrinsic recalcitrance to conventional therapies, new methods of examining these infections and a new class of antifungal drugs must be explored. 2-Amino-nonyl-6-methoxyl-tetralin muriate (10b), a 2-aminotetralin derivate, was synthesized as a novel chemical structural antifungal agent (Figure 1). In our previous study, we found that 10b had anti-biofilm activity. It has been demonstrated that farnesol was an extracellular quorum sensing molecule in the dimorphic fungus *C albicans*[27], which inhibits the yeast to mycelium dimorphic transition and prevents biofilm formation[28]. Therefore, we selected farnesol as positive control to investigate the effect of 10b on *C albicans* biofilms formation. The aim of the work presented here was to further investigate the mechanism of action of 10b against C *albicans* biofilms at molecular level.

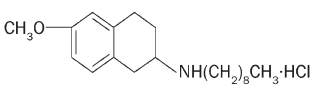

Figure 1. Chemical structure of 2-amino-nonyl-6-methoxyl-tetralin muriate (10b).

Materials and methods

Antifungal agents

Antifunal reagents used in the present experiment included farnesol (Alfa Aesar, A Johnson Matthey Co, Ward Hill, USA); miconazole (MCZ, Pfizer-Roerig Pharmaceuticals, New York, USA); 10b (Department of Medicinal Chemistry, School of Pharmacy, Second Military Medical University, Shanghai, China); and stock solutions of various concentrations in methanol (Sigma).

C albicans strains and growth conditions

C albicans SC5314 was used throughout this study. *C albicans* cells were propagated in yeast-peptone-dextrose (YPD) medium (1% *w/v* yeast extract, 2% *w/v* peptone, 2% *w/v* dextrose). Blastospores were harvested and washed twice in 0.15 mol/L phosphate-buffered saline (PBS; pH 7.2). The cells were then suspended in RPMI-1640 medium (RPMI 1640 supplemented with *L*-glutamine and buffered to pH 7.0 with morpholinepropanesulfonic acid (MOPS)) and counted in a haemocytometer and adjusted to 1.0×10^6 colony forming unit (CFU) /mL.

In vitro anti-biofilm activity assay

C albicans bioflm metabolic activity was assessed using the XTT reduction assay as described previously[29]. The principle is based upon the reduction of tetrazolium to tetrazolium formazan by mitochondrially active yeasts in the presence of menadione, an electron-coupling agent. Briefly, XTT (Sigma Chemical Co) at 0.5 mg/mL was added with menadione (10 mmol/L in acetone) to a final concentration of 1 μmol/L in PBS. A 200 μL aliquot of XTT-menadione was added to each well and incubated in the dark at 37 °C for 2 h. Any colorimetric change (a direct reflection of metabolic activity of the biofilms) was measured in a microtitre plate reader (Multiskan MK3) at 492 nm.

Biofilms were formed in selected 96-microtitre plates. Following the initial 1 h adhesion, the medium was aspirated and then washed thoroughly twice with sterile PBS before the addition of fresh RPMI-1640 medium containing different concentrations of antifungal agents and incubated for another 48 h at 37 °C. A series of antifungal-free wells was also included as controls. Sessile MIC_{50} were determined at 50% inhibition ($SMIC_{50}$) compared with drug-free control wells using XTT reduction assay.

To determine the effect of 10b on adhesion of planktonic cells, antifungal drugs were added to a standardized suspension at zero time (preincubation) before it was added to a 96-microtiter plate. The plate was incubated for 90 min at 37 °C. Knowing that adherent populations on the substratum do not form a structurally differentiated community (biofilm) during this period of time[30], we chose 90 min as the incubation time of the adhesion assay. To determine the effect of 10b on mature biofilms, mature biofilms (48 h) formed as above in the absence of antifungal drugs were added with fresh RPMI-1640 medium containing different concentrations of antifungal drugs. The plates were incubated at 37 °C for 3, 6, 12, and 24 h.

Confocal laser scanning microscopy

Confocal laser scanning microscopy (CLSM) was performed as described in the literature[31] to demonstrate the inhibitory effect of 10b on biofilm formation. Formation of *C albicans* SC5314 biofilms was achieved by adding 4 mL standardized cell suspension to six-well plates containing plastic disks. Following 10b exposure and biofilm formation, the disks were removed and transferred to new six-well culture plates and incubated for 45 min at 37 °C in 4 mL PBS containing the fluorescent stains FUN-1 (10 μmol/L; Molecular Probes, Eugene, Oreg) and concanavalin A–Alexa Fluor 488 conjugate (ConA; 25 μg/mL; Molecular Probes). FUN-1 (excitation wavelength, 543 nm; emission wavelength, 560 nm; long-pass filter) is converted to an orange-red cylindrical intravacuolar structure by metabolically active cells, while ConA (excitation

wavelength, 488 nm; emission wavelength, 505 nm; long-pass filter) binds to glucose and mannose residues of cell wall polysaccharides and emits a green fluorescence. After incubation with the dyes, the disks were flipped and the stained biofilms were observed with a Leica TCS sp2 CLSM equipped with argon and HeNe lasers.

RNA isolation and microarray hybridization

For RNA isolation experiments, cells were added to 25 mL portions of RPMI-1640 medium in 75-cm^2 tissue culture flasks with vented caps. The flasks were incubated statically for 1 h to allow initial adherence of the cells, and then the medium was decanted and replaced with 25 mL portions of fresh RPMI-1640 medium containing 10 μmol/L 10b. We chose this 10b concentration because it still maintained an inhibitory effect on biofilm formation and allowed for recovery of a sufficient cellular mass for RNA extraction. The flasks were then incubated statically for 48 h at 37 °C. A 10b-free control was also included. Total RNA was isolated by the hot phenol method[32] and purified with a NecleoSpin® Extract II kit (Machery-Nagel Corp, Germany) following the manufacturer's protocol. A 7925 C *albicans* genome 70-mer oligonucleotide microarray was obtained from CapitalBio Corporation (Beijing, China). A 1-μg sample of total RNA was used for preparing fluorescent dye-labeled cDNA by the linear mRNA amplification procedure as described[33]. A DNA–DNA hybridization protocol was used to replace RNA–DNA hybridization in the present study for the sake of reducing cross-hybridization[34]. The labeled cDNAs were dissolved in 80 μL hybridization solution [3×SSC, 0.2% (*w/v*) SDS, 5× Denhardt's solution, 25% (*v/v*) formamide] and denatured at 95 °C for 3 min before hybridization. A sample of the mixed hybridization buffer was placed onto a microarray slide and covered with a glass coverslip. Hybridization was done with a BioMixer™ II (CapitalBio Corp, China). After hybridization, the slides were washed with washing solution 1 (2×SSC, 0.2% SDS) and then with washing solution 2 (2×SSC) at 42 °C for 4 min. Self-hybridization of the control sample was used to evaluate the system noise.

The microarrays were scanned with a LuxScan™ 10KAscanner (CapitalBio Corp, China) at two wavelengths to detect emissions from both Cy3 and Cy5. The image obtained was analyzed with LuxScan™ 3.0 software (CapitalBio Corp, China). Normalization was done on the basis of a Lowess program[35]. The ratio of Cy5 to Cy3 was calculated for each location on each microarray. To minimize artifacts that arose from low expression values, only genes with raw intensity values>800 counts for both Cy3 and Cy5 were chosen for analysis. A "one class" method for the analysis of microarray software (SAM) was used to identify significantly differentially expressed genes. Genes with a false discovery rate (FDR)<5%, *q*-value <1% and variation of at least 2-fold in SC5314 biofilms following 10b exposure were identified as significantly differentially expressed genes in two independent experiments. Differentially expressed genes were clustered hierarchically by Gene Cluster 3.0 (Stanford University). DNA sequences were annotated on the basis of the results of BlastN and BlastX searches using the sequencing database of Stanford University (Palo Alto, CA) (http://www-sequence.stanford.edu/group/candida/), GenBank (http://www.ncbi.nlm.nih.gov/BLAST/), and CandidaDB database (http://genolist.pasteur.fr/CandidaDB/).

The entire arrary data have been deposited in the NCBI gene Expression Omnibus (GEO) (http://www. ncbi.nlm.nih.gov) and are aceesible through GEO series accession number GSE19226.

Quantitative real-time RT-PCR assay

Real-time RT-PCR was used to confirm microarray results of gene expression changes. An aliquot of the RNA preparations used in the microarray experiments was saved for this follow-up study. Moreover, duplicate independent experiments were conducted to isolate RNA samples according to the protocol described above. First-strand cDNAs were synthesized from 1 μg total RNA in a 20 μL reaction volume using the cDNA synthesis kit for RT-PCR (TaKaRa Biotechnology, Dalian, China) in accordance with the manufacturer's instructions. Real-time PCR reactions were performed with SYBR Green I (TaKaRa), using ABI 7500 Real-Time PCR system (Applied Biosystems Co, California, USA). Gene-specific primers were designed using Discovery Studio Gene software (Accelrys, Inc). The thermal cycling conditions comprised an initial step at 95 °C for 1 min, followed by 40 cycles at 95 °C for 10 s, 55 °C for 20 s, and 72 °C for 30 s. Change in SYBR Green I fluorescence in every cycle was monitored by the system software, and the threshold cycle (C_T) was measured. Using 18S rRNA as the internal control, gene expression of SC5314 biofilms treated by 10b relative to that without treatment was calculated using the formula $2^{-\triangle\triangle CT}$, where $\triangle C_T$ is the C_T value of genes of interest minus that of the internal control, and $\triangle\triangle C_T$ is the mean $\triangle C_T$ value of SC5314 biofilms treated by 10b minus that without treatment. Primer sequences used in real-time RT-PCR assay are listed in Table 1.

Statistics

Experiments were performed at least three times. Data are presented as 'mean±standard deviations' and analyzed using the Student's *t* test where indicated.

Results

In vitro anti-biofilm activity of 10b

10b had been reported to have great antifungal activity[36, 37], but its dramatic anti-biofilm activity was unexpected. CLSM showed that normal *C albicans* biofilm exhibited a typical three-dimensional structure and composed mainly of true hyphae and pseudohyphae (Figure 2A). When cells were preincubated with 10 μmol/L farnesol at 0 h incubation time, biofilm development can not be prevented and still composed mainly of true hyphae and pseudohyphae (Figure 2B). However, after preincubation with 0.1 μmol/L 10b, the typical architecture of biofilms (intertwining mycelial structures and a basal layer of blastospores) was destructed although

Table 1. List of primers used for real-time RT-PCR.

Target genes	Primer pairs (5′–3′)[a)]	Amplicon size (bp)
18s	(F) TCTTTCTTGATTTTGTGGGTGG	
	(R) TCGATAGTCCCTCTAAGAAGTG	150
ECE1	(F) TGACCAAGCACCTACT	
	(R) AGCAATGATACCAGCA	190
NRG1	(F) CCATCTCCAGGGCTAAT	
	(R) TTCTTCTTGGGTCTTTG	139
CSA1	(F) TCTCAAGTTCCACAAG	
	(R) GGTAGAGTTTCCGTAG	267
ACE2	(F) ACTGCTTTCCCATCCTAT	
	(R) TAATCCCATCAATGTTTC	215
BMT9	(F) TGCTTCTGGCAAGTCAA	
	(R) TTCCCCTCACATAATCC	105
FGR6-10	(F) ACAGTTCTTCGTTTCGG	
	(R) TGGTTGGTGTCTCGTTG	157
SFL1	(F) CCCCTCAATCGTCATAC	
	(R) TGCAGCTCCAGAAGTAG	200
ADH1	(F) ATCCCTGGTCTTATCTTC	
	(R) AACTGGGTAATCCTTGTAG	184
HXK2	(F) CGGTTACTATTTGGGAGA	
	(R) TTGGATGGATAAGAGGC	132
CDC19	(F) CTGCTGCTTACGAACA	
	(R) AATGGGTAGACACCTCTG	163
PFK1	(F) AGAAACCTGCCTCCTCA	
	(R) CCAACCCTAATCTGTCG	177
GPX2	(F) ACTCCACAATACAAAGGTT	
	(R) AATACGGGGAAAGTCAC	164
SOD5	(F) ACATTGGCGGTTTATC	
	(R) ATTACCTTGAGGAGCA	185
SOD2	(F) AACTTGGCTCCTGTCTC	
	(R) TATCACCATTGGCTTTG	181
XOG1	(F) TCCAAGTCTTTGGCTAT	
	(R) ACTGAAATGTGGTCGTT	133
SLD1	(F) AGATAGAAGGACCAAGA	
	(R) GGAACAAACCCAATACC	224
DAG7	(F) AAAGGTAACACTAAGATTC	
	(R) GTAAAAGTTGTAGATGGG	119
SFL2	(F) TGGGTTCCATAAAGTGAG	
	(R) ATAGGTTCGGCATAGATT	213
GZF3	(F) AGTCAAACAAAATGGAAGC	
	(R) TTGCCTGATTTGCCTTC	90
ERG2	(F) GTCTAATGACCCAGTTGT	
	(R) TCTTCTTCTGCCTTTGCA	162
ERG6	(F) GCTACCGTTCATGCTCCA	
	(R) CCATCACCGACTTCAATA	164
ERG11	(F) GAATCCCTGAAACCAAT	
	(R) AGCAGCAGTATCCCATC	131
ERG24	(F) GGTGACTTAGCGTGGGT	
	(R) GCTGAGCGGAAGATGTA	143

[a)] F, forward; R, reverse.

pseudohyphae and true hyphae were observed (Figure 2C). Moreover, the concentration was increased by 10-fold, the adherent yeast cells were successfully prevented from germination and resulted in scant or nonexistent biofilms (Figure 2D). Effect of 10b on biofilm formation was also assessed by XTT reduction assay as seen in Figure 3. Over 90% inhibition of biofilm formation was observed at 10b concentrations over 15.63 μmol/L. Lower concentrations (7.81 to 15.63 μmol/L) produced about 50% inhibition. Moreover, 10b used at 1.95 to 3.91 μmol/L was still able to reduce about 30%–40% metabolic activity (Figure 3A). Farnesol was also able to inhibit biofilm formation to some extent but the inhibitory effect was relatively poor (Figure 3B). Less than 55% inhibitory efficiency of biofilm formation was observed at farnesol concentrations over 15.63 μmol/L. No significant inhibition was observed at farnesol concentrations lower than 7.81 μmol/L. Furthermore, the $SMIC_{50}$ value of 10b and farnesol were 7.05 μmol/L and 187.50 μmol/L, respectively, as determined by XTT reduction assay.

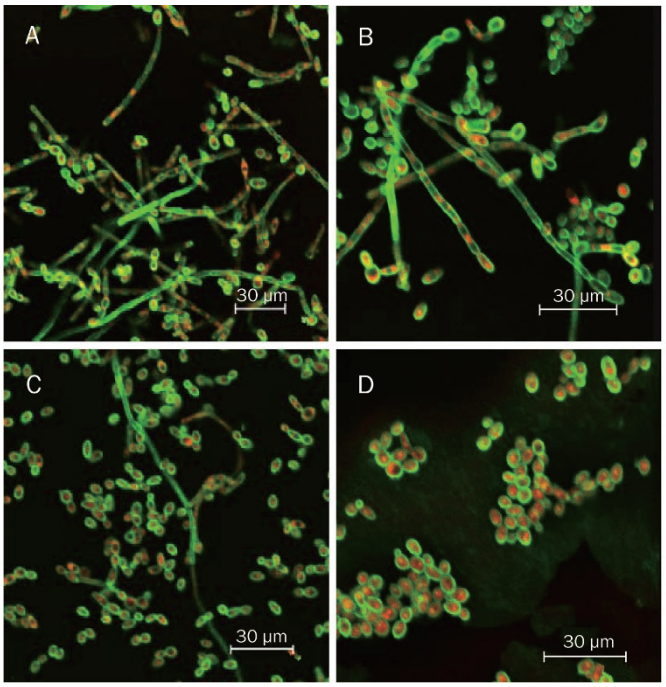

Figure 2. Morphology alteration of *C albicans* strain after treated with 10b. Confocal laser scanning microscopy of *C albicans* biofilms: (A) normal biofilm; (B) cells treated with 10 μmol/L farnesol at 0 h of the incubation time; (C) cells treated with 0.1 μmol/L 10b at 0 h of the incubation time; (D) cells treated with 1.0 μmol/L 10b at 0 h of the incubation time.

Next, mature (48 h) biofilms were added with fresh growth medium containing 10b and farnesol, and incubated for another 3 to 24 h. As seen in Table 2, 10b at 10 and 50 μmol/L were able to markedly inhibit the metabolic activity of mature biofilms whenever 10b was added. Moreover, 10b at 50 μmol/L was able to achieve 62.71% inhibitory efficiency after incubation for 24 h. However, only farnesol at 50 μmol/L was able to inhibit metabolic activity of mature biofilms significantly. It was worth mentioning that extension of the incubation time increased the efficiency of 10b and farnesol in inhibiting the metabolic activity of mature biofilms.

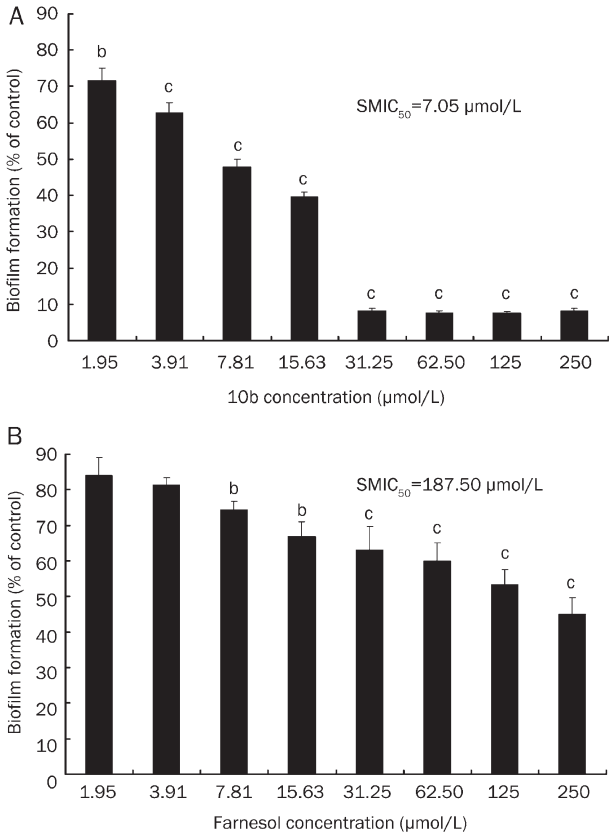

Figure 3. Inhibition of biofilm formation by different concentrations of 10b (A) and farnesol (B). Biofilm formation (as measured by XTT reduction) is expressed as a percentage of control biofilms. The data are expressed as mean±standard deviation (SD) of three independent experiments. The mean±SD of the mean control values (A_{492}) was 1.083±0.056. Statistically significant differences as determined by Student's *t* test. $^{b}P<0.05$, $^{c}P<0.01$ *vs* control.

Gene expression responses to 10b exposure

To reveal the mechanism of 10b against biofilms at the molecular level, *C albicans* cDNA microarrays were used to identify changes in gene expression profiles of *C albicans* SC5314 biofilms following 10b exposure in two independent experiments. To avoid dye-associated effects on cDNA synthesis, RNA from the 10b-treated group was labeled with Cy5 and Cy3 separately. In each hybridization experiment, duplicate spots were measured as usual. After statistical analysis of six individual comparisons, only the statistically significant (FDR<5%, *q*-value<1%) genes whose expression level changed by at least 2-fold in all data sets were selected. The data generated from these independent microarray experiments reflected a high level of reliability and reproducibility due to the presented ratios obtained from repeated assays of the same samples and of samples from the independent experiments.

A total of 149 differentially expressed genes were found upon exposure to 10b, of which 69 genes showed a decrease in expression, and 80 genes showed an increase in expression (Table 3 and 4). Ten differentially expressed genes were found to relate to biofilm formation, filamentous or hyphal growth. It was noticed that striking up-regulation of *NRG1* and marked down-regulation of *ECE1* directly related to the inhibition of biofilm formation. One gene related to specifically hydrolyzing beta-1,3 glucan (*XOG1*) was significantly increased. Ten down-regulated genes were involved in glycolysis (*eg, HXK2*), fermentation (*eg, ADH1*) and active oxygen scavenging (*eg, SOD5*). Fifteen overexpressed genes were related to the lipid metabolic process. Of them, 13 genes were directly linked to ergosterol biosynthesis, including *ERG2, ERG6* and *ERG11*. Ten genes related to translation were overexpressed following exposure to 10b. Of them, 2 genes involved in negative regulation of transcription were significantly up-regulated.

Validation of microarray data by real-time RT-PCR

To validate the expression of genes identified by microarray analysis, real-time RT-PCR was perfomed in 23 genes of interest selected on the basis of their roles in the specific action mechanism of 10b (*eg, ECE1, NRG1, CSA1, ACE2, BMT9, FGR6-10, SLF1, ADH1, HXK2, CDC19, PFK1, GPX2, SOD5, SOD2* and *XOG1*) and in the responses independent of mechanism of action (*eg, SLD1, DAG7, SFL2, GZF3, ERG2, ERG6, ERG11* and *ERG24*). Total RNA samples from cells treated or untreated with 10b were prepared in parallel for three separate experiments. Real-time RT-PCR reactions were performed in triplicate with independent RNA isolations. It was found that the expression of gene *PFK1* was down-regulated as shown by real-time RT-PCR in three independent experiments. In general, there was a good correlation between real-time RT-PCR

Table 2. Effects of 10b and farnesol incubated for different times on mature (48 h) biofilms.

Drugs incubation time (h)	XTT reduction (%) [a] after further incubation in medium containing compounds at the concentration of:			
	10b		Farnesol	
	10 μmol/L	50 μmol/L	10 μmol/L	50 μmol/L
3	76.68±4.52^{b}	60.35±6.17^{c}	108.13±6.34	79.14±6.70
6	73.61±3.21^{b}	51.43±7.81^{c}	110.47±10.74	69.23±1.47^{b}
12	62.41±5.27^{c}	47.06±6.37^{c}	97.11±6.01	71.58±1.76^{b}
24	58.19±2.51^{c}	37.29±3.18^{c}	98.73±7.05	64.72±5.97^{c}

a) 10b and farnesol were added to mature (48 h) biofilms and incubation was continued for further 3 to 24 h at 37 °C. XTT reduction is expressed as a percentage of that of control mature biofilms (48 h) further incubated for the same time period without the above drugs. The results are mean±standard deviations of three independent experiments. $^{b}P<0.05$, $^{c}P<0.01$ *vs* control.

Table 3. Genes down-regulated in 10b-grown biofilms compared to biofilms without treatment through two independent experiments.

Primary CGDID	Gene name (CandidaDB)	*S cerevisiae* homologue name	Function	Change in fold expression Ratio1	Ratio2
Biofilm formation					
CAL0004191	*ECE1*	None	Extent of cell elongation	0.10	0.10
CAL0002846	*CSA1*	YIR019C	Candida Surface Antigen	0.39	0.23
CAL0005982	*ACE2*	YLR131C	Transcription activator activity	0.32	0.40
CAL0003176	*ADH1*	YOL086C	Alcohol dehydrogenase	0.35	0.45
Filamentous growth					
CAL0003785	*BMT9*	None	Wild-type filamentous growth	0.47	0.24
CAL0001036	*GIN1*	YCL061C	Regulation of DNA-damage-induced filamentous growth	0.41	0.43
CAL0002878	*FGR6-10*	YNR044W	Filamentous Growth Regulator	0.41	0.37
Cell budding					
CAL0001436	*ATS1*	YAL020C	Induced upon adherence to polystyrene	0.39	0.32
Generation energy					
CAL0003653	*IFE2*	YAL060W	(*R*,*R*)-butanediol dehydrogenase activity	0.29	0.25
Glycolysis					
CAL0000415	*PGK1*	YCR012W	PhosphoGlycerate Kinase	0.38	0.46
CAL0005657	*TDH3*	YGR192C	Triose phosphate DeHydrogenase	0.42	0.37
CAL0002184	*PGI1*	YBR196C	Glucose-6-phosphate isomerase activity	0.33	0.39
CAL0003176	*ADH1*	YOL086C	Alcohol dehydrogenase	0.35	0.45
CAL0002618	*SAD2*	YOL086C	Alcohol dehydrogenase (NAD) activity	0.44	0.46
CAL0000198	*HXK2*	YGL253W	Hexokinase II	0.43	0.37
CAL0003055	*PFK1*	YGR240C	Alpha subunit of phosphofructokinase (PFK)	0.49	0.65*
Protein degradation					
CAL0006261	*SAP5*	YIL015W	Secreted aspartyl proteinase	0.23	0.29
CAL0001377	*SAP4*	YLR121C	Secreted aspartyl proteinase	0.30	0.32
Protein modification process					
CAL0005317	*RAM2*	YKL019W	Geranylgeranyltransferase and farnesyltransferase	0.37	0.29
Amino metabolic					
CAL0000320	*PUT1*	YLR142W	Proline dehydrogenase activity	0.33	0.26
CAL0004575	*CBP1*	YJL209W	Corticosteroid binding protein	0.47	0.23
CAL0001679	*ARO10*	YDR380W	Phenylpyruvate decarboxylase activity	0.38	0.23
CAL0001524	*RNR1*	YER070W	Ribonucleoside-diphosphate reductase activity	0.39	0.39
CAL0005223	*PRI2*	YKL045W	DNA replication initiation	0.45	0.48
CAL0002119	*SIS1*	YNL007C	Protein complex assembly	0.43	0.41
CAL0004541	*UGA33*	YDR207C	Predicted zinc-finger protein of unknown function	0.49	0.39
Transport					
CAL0001208	*SSA2*	YLL024C	HSP70 family chaperone	0.28	0.29
CAL0003217	*OPT4*	YPR194C	Oligopeptide transporter	0.22	0.04
CAL0001762	*CDR4*	YOR153W	ATP-binding cassette (ABC) superfamily	0.28	0.25
CAL0003136	*MAL31*	YBR298C	Sugar transmembrane transporter activity	0.35	0.27
CAL0004351	*HGT6*	YDR343C	Glucose transmembrane transporter activity	0.34	0.37
CAL0005849	*HGT15*	YOL103W	Glucose transmembrane transporter activity	0.31	0.40
CAL0002675	*GIT2*	YCR098C	Inorganic phosphate transmembrane transporter activity	0.46	0.33
CAL0002987	*CFL2*	YNR060W	Ferric-chelate reductase activity	0.24	0.33
CAL0002260	*ARR3*	YPR201W	Arsenite transmembrane transporter activity	0.50	0.33
CAL0003283	*TNA12*	YGR260W	Putative transporter	0.32	0.15
CAL0002083	*DIP53*	YPL265W	Amino acid transmembrane transporter activity	0.33	0.07
CAL0004943	*ENT4*	YLL038C	Endocytosis	0.35	0.29
CAL0002211	*IPF17497.2*	YDL058W	ER to Golgi vesicle-mediated transport	0.43	0.18
CAL0001603	*TIF6*	YPR016C	Ribosome export from nucleus	0.45	0.45
Cell stress					
CAL0001501	*CDC1*	YDR182W	Cellular metal ion homeostasis	0.48	0.35
CAL0004229	*RPH1*	None	DNA repair	0.45	0.28
CAL0002987	*CFL2*	YNR060W	Ferric-chelate reductase activity	0.24	0.33
CAL0002431	*POL1*	YNL102W	DNA-directed DNA polymerase activity	0.30	0.33
CAL0006305	*MSH6*	YDR097C	Involved in mismatch repair	0.41	0.35

(Continued)

Primary CGDID	Gene name (CandidaDB)	*S cerevisiae* homologue name	Function	Change in fold expression Ratio1	Ratio2
CAL0001410	*HSP104*	YLL026W	ATPase activity	0.28	0.23
Response to oxidative stress					
CAL0006314	*ZTA1*	YBR046C	Similar to quinone oxidoreductases	0.32	0.19
Active oxygen scavenging					
CAL0004456	*SOD5*	None	Copper- and zinc-containing superoxide dismutase	0.17	0.12
CAL0004253	*AHP1*	YLR109W	Putative alkyl hydroperoxide reductase	0.36	0.49
Lipid metabolic process					
CAL0000982	*FDH1*	Y0R388C	Formate dehydrogenase activity	0.36	0.08
CAL0000562	*AYR2*	YIL124W	Acylglycerone-phosphate reductase activity	0.46	0.45
CAL0001801	*SOU3*	YNL202W	2,4-dienoyl-CoA reductase (NADPH) activity	0.49	0.42
Vitamin metabolism					
CAL0002332	*IPF21405.1*	YMR289W	Folic acid biosynthetic process	0.40	0.48
Carbohydrate metabolic					
CAL0004557	*DAK2*	YFL053W	Glycerone kinase activity	0.34	0.43
Not classified					
CAL0000985	*XYL2*	YJR159W	Xylose degradation	0.29	0.08
CAL0006015	*BUD20*	YLR074C	Cellular bud site selection	0.35	0.43
CAL0006205	*IPF22400.1*	*YCR062W*	Regulation of cell size	0.40	0.41
CAL0001631	*RIM1*	YCR028C-A	Mitochondrial genome maintenance	0.46	0.49
Unknown function					
CAL0002175	*IPF525.1*	YAL035W	Unknown	0.19	0.13
CAF0006968	*IPF10241.3*	None	Unknown	0.21	0.22
CAL0001404	*ALK1*	YDR402C	Unknown	0.23	0.21
CAL0004116	*IPF27058.1*	None	Unknown	0.32	0.36
CAL0003595	*IPF22624.1*	YAL049C	Unknown	0.33	0.19
CAL0004079	*IPF19669.1*	None	Unknown	0.35	0.29
CAF0007012	*IPF22833.1*	None	Unknown	0.36	0.24
CAF0007044	*IPF21764.1*	None	Unknown	0.38	0.20
CAL0004085	*IPF27036.1*	None	Unknown	0.40	0.48
CAL0005268	*IPF21758.1*	None	Unknown	0.40	0.18
CAL0004173	*IPF10394.1*	None	Unknown	0.38	0.37

* Real-time RT-PCR verified the expression of the gene down-regulation through three independent experiments.

and microarray data (Figure 4).

Effects of ROS on *C albicans* biofilms

According to Pastuer effect, the tricarboxylic acid cycling process might be enhanced because the expression of genes participating in glycolysis was decreased after exposure to 10b under aerobic circumstances. Besides, the expression of genes encoded superoxide dismutase (SOD) was also decreased. This might result in augmentation of ROS generation (Figure 5). To assess the role of endogenous ROS against *C albicans* biofilms, XTT reduction assay was performed to investigate the effects of ROS scavenger, ascorbic acid (AA), on anti-biofilm activity of 10b with respect to planktonic cell adhesion, biofilm formation and mature biofilm (48 h) metabolic activity. Table 5 shows that 10b+AA or 10b alone had no effect on planktonic cell adhesion although 10b+AA notably increased metabolic activity of planktonic cells compared to 10b (P<0.01). No significant difference between 10b+AA and 10b was found in inhibitory efficiency of biofilm formation despite the fact that 10b+AA markedly inhibited biofilm formation compared to AA (P<0.01) (Table 6). 10b+AA significantly increased mature biofilm metabolic activity compared to 10b (P<0.05) (Table 6). These results indicated that endogenous ROS augmentation generated by 10b is a pivotal action mechanism to reduce mature biofilm metabolic activity, although elevated endogenous ROS have no impact upon biofilm formation and planktonic cell adhesion. To further verify above conclusion, XTT reduction assay was performed to investigate the effect of a well known ROS inducer MCZ on mature biofilm metabolic activity. As expected, MCZ at 10 μmol/L and 50 μmol/L markedly decreased mature biofilm metabolic activity and the inhibitory efficiency was 39.08% and 58.68%, respectively, after 6 h exposure (Figure 6). Our data further confirmed a direct correlation between endogenous ROS augmentation and inhibition of mature biofilm metabolic activity.

Discussion

10b is a novel chemical structural antifungal agent with high antifungal activity, a broad antifungal spectrum and potentially low toxicity[36, 37]. In this study, we found that 10b

Table 4. Genes up-regulated in 10b-grown biofilms compared to biofilms without treatment through two independent experiments.

Primary CGDID	Gene name	*S cerevisiae* homologue name	Function	Change in fold expression Ratio1	Ratio2
Translation					
CAL0004848	*GAT2*	YMR136W	Transcription factor activity	2.43	2.94
CAL0003471	*TEF4*	YKL081W	Putative translation elongation factor	3.93	2.14
CAL0004558	*TEF2*	YBR118W	Translation elongation factor activity	2.26	2.21
CAL0001367	*SSB1*	YDL229W	Putative heat shock protein	2.01	2.91
CAF0007000	*RPL43A*	YJR094W-A	Predicted ribosomal protein	3.19	2.33
CAL0003667	*RPL20B*	YMR242C	Predicted ribosomal protein	2.25	2.11
CAL0005037	*RPL10A*	YGL135W	Predicted ribosomal protein	2.92	2.53
CAL0003534	*NAN1*	YPL126W	Positive regulation of transcription	2.09	3.02
CAL0001506	*UBI3*	YLR167W	Structural constituent of ribosome	2.31	2.09
CAL0004215	*SEN2*	YLR105C	tRNA-intron endonuclease activity	3.07	3.57
CAL0003059	*SFL2*	YOR140W	Negative regulation of transcription	6.19	4.54
CAL0005136	*GZF3*	YJL110C	Negative regulation of transcription	3.83	20.63
DNA metabolic					
CAL0006292	*POL5*	YEL055C	DNA-directed DNA polymerase activity	3.10	6.48
RNA metabolic					
CAL0002072	*GAR1*	YHR089C	Box H/ACA snoRNA binding	2.32	2.75
CAL0001653	*CBF5*	YLR175W	Pseudouridylate synthase activity	2.42	2.69
CAL0001648	*TRM3*	YDL112W	tRNA (guanine) methyltransferase activity	2.34	2.72
CAL0002141	*TSR1*	YDL060W	rRNA processing	2.26	3.16
CAL0005606	*RRP5*	YMR229C	Poly(U) RNA binding	2.23	6.85
Transport					
CAL0006337	*MEP1*	YPR138C	Ammonium transmembrane transporter activity	3.70	4.47
CAL0001711	*VPS11*	YMR231W	Vacuolar protein sorting	3.46	3.08
CAL0003818	*HGT17*	YNR072W	Putative glucose transporter	3.77	4.59
CAL0001467	*HGT10*	YDR536W	Glycerol permease	6.16	2.92
CAL0003382	*CDR2*	YOR153W	Multidrug transporter	4.64	3.24
CAL0006143	*FEN2*	YCR028C	Predicted membrane transporter,	3.86	3.45
Cell wall maintenance					
CAL0006153	*XOG1*	YLR300W	Exo-1,3-beta-glucanase, major exoglucanase	3.02	8.78
CAL0000069	*MNT2*	YDR483W	Alpha-1,2-mannosyl transferase	2.06	2.19
CAL0001642	*SIM1*	YKR042W	Cell wall organization	4.03	4.47
CAL0002002	*PHR1*	YMR307W	Glycosidase of cell surface	2.05	2.34
Hyphal or filamentous growth					
CAL0002995	*NRG1*	YPR015C	Transcriptional repressor, regulates hyphal genes	5.13	3.96
CAL0004265	*FGR29*	None	Filamentous growth regulator	2.51	3.10
CAL0002268	*CZF1*	YDR207C	C albicans Zinc Finger protein, hyphal growth regulator	2.89	4.33
Cell cycle					
CAL0004825	*ULP1*	YPL020C	G_2/M transition of mitotic cell cycle	2.37	2.61
Lipid metabolic process					
CAL0004027	*SLD1*	None	SphingoLipid delta-8 Desaturase	5.12	9.78
CAL0006277	*FAD3*	None	Omega-3 fatty acid desaturase activity	2.42	3.32
CAL0000316	*ERG9*	YHR190W	Farnesyl-diphosphate farnesyltransferase	9.40	9.17
CAL0006397	*ERG6*	YML008C	Sterol 24-C-methyltransferase	22.68	13.02
CAL0002665	*ERG5*	YMR015C	C-22 sterol desaturase	7.65	26.93
CAL0001905	*ERG3*	YLR056W	C-5 sterol desaturase	3.37	5.56
CAL0003306	*ERG27*	YLR100W	3-keto sterol reductase	2.98	5.53
CAL0005951	*ERG26*	YGL001C	C-3 sterol dehydrogenase (C-4 sterol decarboxylase)	5.45	10.31
CAL0003665	*ERG251*	YGR060W	C-4 methylsterol oxidase	10.11	16.52
CAL0001165	*ERG25*	YGR060W	C-4 methylsterol oxidase	6.03	9.31
CAL0005685	*ERG24*	YNL280C	Delta14-sterol reductase	6.08	6.95
CAL0005073	*ERG2*	YMR202W	C-8 sterol isomerase	31.41	18.07
CAL0004537	*ERG13*	YML126C	Hydroxymethylglutaryl-CoA synthase	3.52	11.90
CAL0003627	*ERG11*	YHR007C	Lanosterol 14-alpha-demethylase	7.74	16.75
CAL0005541	*ERG1*	YGR175C	Squalene epoxidase	5.21	5.14

(Continued)

Primary CGDID	Gene name	*S cerevisiae* homologue name	Function	Change in fold expression Ratio1	Ratio2
Amino acid metabolic					
CAL0001464	*SHM2*	YLR058C	Cytoplasmic serine hydroxymethyltransferase	2.37	2.92
CAL0002855	*SAH1*	YER043C	S-adenosyl-*L*-homocysteine hydrolase	3.95	4.90
CAL0004803	*ILV3*	YJR016C	Dihydroxy-acid dehydratase activity	2.52	2.09
CAL0003242	*HIS3*	YOR202W	Imidazoleglycerol-phosphate dehydratase	2.19	5.21
CAL0004374	*GDH3*	YAL062W	Glutamate dehydrogenase (NADP+) activity	3.80	3.71
CAL0004920	*GCV2*	YMR189W	Glycine dehydrogenase (decarboxylating) activity	2.02	8.86
CAL0006098	*GCV1*	YDR019C	T subunit of glycine decarboxylase	2.25	9.99
CAL0002497	*CDC60*	YPL160W	Cytosolic leucyl tRNA synthetase	2.08	2.36
CAL0006284	*SPE3*	YPR069C	Spermidine synthase activity	2.48	2.11
CAL0002778	*UGA11*	YGR019W	4-aminobutyrate transaminase activity	2.31	2.11
CAL0006381	*IPF25064.1*	YJR070C	Deoxyhypusine monooxygenase activity	2.06	5.86
CAL0003436	*HMT1*	YBR034C	HnRNP MethylTransferase	2.20	3.48
Generation energy					
CAL0006095	*ADH7*	YCR105W	Similar to alcohol dehydrogenases	2.85	3.98
Protein modification process					
CAL0003800	*SET3*	YKR029C	NAD-dependent histone deacetylase activity	5.07	3.84
Carbohydrate metabolic process					
CAL0000604	*RHD1*	None	Putative beta-mannosyltransferase	6.04	3.70
Cell stress					
CAL0001195	*PGA23*	YFL067W	Putative GPI-anchored protein of unknown function	2.61	3.60
CAL0003828	*DAG7*	None	Response to drug	13.05	8.15
CAL0000509	*IMH3*	YML056C	Inosine monophosphate (IMP) dehydrogenase	2.44	3.41
CAL0001161	*GPD2*	YDL022W	Intracellular accumulation of glycerol	2.66	3.07
Cell adhesion					
CAL0005516	*AAF1*	YKL054C	Possible regulatory protein	3.63	2.27
Protein degradation					
CAL0002041	*SAP10*	YDR144C	Secreted aspartyl proteinase	2.92	2.25
Not classified					
CAL0003017	*IPF26080.1*	YGR111W	Regulation of cell size	2.09	3.24
CAL0006203	*IPF17082.3*	YNL176C	Fungal-type vacuole	2.06	3.77
Unknown					
CAL0004126	*IPF7374.2*	None	Unknown	15.24	10.30
CAL0003826	*IPF26000.1*	None	Unknown	13.89	13.02
CAL0003064	*IPF26046.1*	None	Unknown	8.75	5.53
CAL0000188	*IPF19200.1*	YNR018W	Unknown	6.14	5.01
CAL0000394	*IPF2997.1*	None	Unknown	6.02	2.44
CAL0003899	*IPF27112.1*	YPR013C	Unknown	5.77	15.00
CAL0001181	*IPF22876.1*	None	Unknown	4.03	2.42
CAL0005757	*IPF20288.1*	None	Unknown	3.41	4.38
CAL0001538	*AM01*	None	Unknown	3.12	3.47
CAL0000702	*IPF9592.2*	YFL043C	Unknown	3.11	3.35

had strong anti-biofilm activity. To further investigate the action mechanism, cDNA microarray study was performed in *C albicans* SC5314 biofilms treated or untreated with 10b. The results of real-time RT-PCR showed that differentially expressed genes were involved in multiple biochemical functions. Our particular interest was the striking changes of biofilm formation related genes and energy-metabolism-related genes: glycolysis-related genes, fermentation-related genes and active oxygen scavenging-related genes.

It was found in this study that biofilm formation was directly related to striking down-regulation of *ECE1* and marked up-regulation of *NRG1*. *ECE1*, a hypha-specific gene, is involved in the process of cell extension, the first morphological sign of which is the emergence of a germ tube approximately 90 min after induction[38]. Reports have confirmed that *ECE1* promoter is strongly repressed by Nrg1p, a sequence-specific DNA-binding protein, under non-inducing conditions[39, 40]. Nrg1p, endoed by *NRG1*, plays important roles in the regulation of yeast-hyphal morphogenesis, and represses a subset of Tup1-regulated genes, including known hypha-specific genes and other virulence factors. Most of these genes contain an Nrg1p response element (NRE) in their promoter.

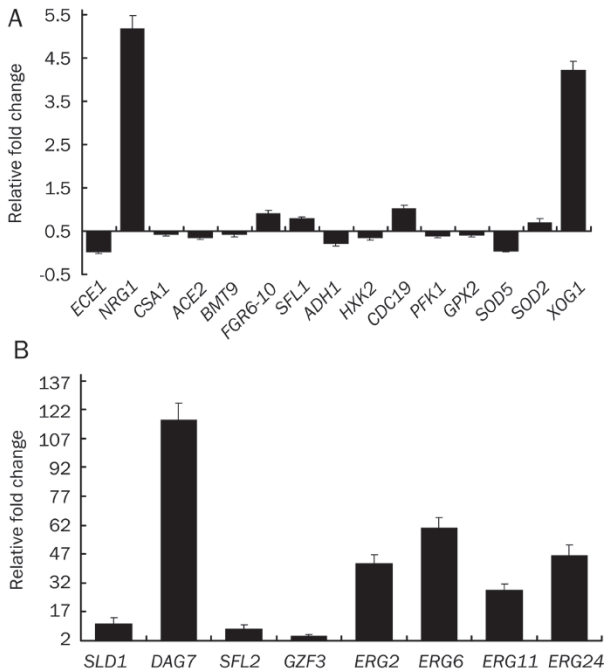

Figure 4. Gene expression changes in 25 genes of interest in *C albicans* SC5314 biofilms treated with 10b (10 μmol/L) relative to untreatment: (A) genes related to the specific action mechanism of 10b; (B) genes independent of the action mechanism of 10b. All the genes were examined by real-time RT-PCR with gene-specific primers.

Nrg1p interacts specifically with an NRE *in vitro*[39]. Inactivation of Nrg1p in *C albicans* causes flamentous and invasive growth, derepresses hypha-specific genes and increases sensitivity to some stresses[39–41]. Our data indicate that striking down-regulation of *ECE1* and marked up-regulation of *NRG1* induced by 10b might play a pivotal role during biofilm formation.

Another interesting result was the change of energy-metabolism-related genes after 10b treatment: global down-regulation of glycolysis-related genes, fermentation-related genes and antioxidant defense genes. According to Pasteur effect that aerobic oxidation could inhibit glycolysis (alcohol-facient fermentation) under aerobic circumstances, the tricarboxylic acid cycling process might be enhanced following exposure to 10b because expression of the genes participating in glycolysis especially encoding two rate-limiting enzymes genes, *HXK2* and *PFK1*, was markedly decreased. Besides, expression of the gene encoded superoxide dismutase (*SOD5*) was also decreased. Together, endogenous ROS generation might be markedly augmented and experiment verified our deduce (data not shown). To determine whether endogenous ROS augmentation was the major mechanism of 10b against *C albicans* biofilms, we performed XTT reduction assay to investigate the effect of anti-oxidant AA on the anti-biofilm activity of 10b and the effect of a well known ROS inducer MCZ on mature biofilm metabolic activity. Taken together, our results suggest that the mechanism of 10b against mature biofilms is associated with the augmentation of endogenous ROS by affecting aerobic respiration in mitochondria.

Endogenous ROS, a natural byproduct of normal cellular metabolism , derives from mitochondrial respiratory chain electron leakage and plays important roles in cellular components damage and DNA cell signaling[42, 43]. Reports have confirmed that increase of intracellular ROS production is involved in the mechanism of several antifungal agents[44, 45]. Furthermore, it was found in our previous study that decreased endogenous ROS generation contributes to drug resistance of *C albicans*[46]. However, the mechanisms by which *Candida* biofilms resist the action of antifungal agents are not known. In our present study, we found that the augmentation of endogenous ROS generated by 10b significantly reduced mature biofilm metabolic activity, and when the augmentation endogenous ROS is scavenged after addition of anti-oxidant

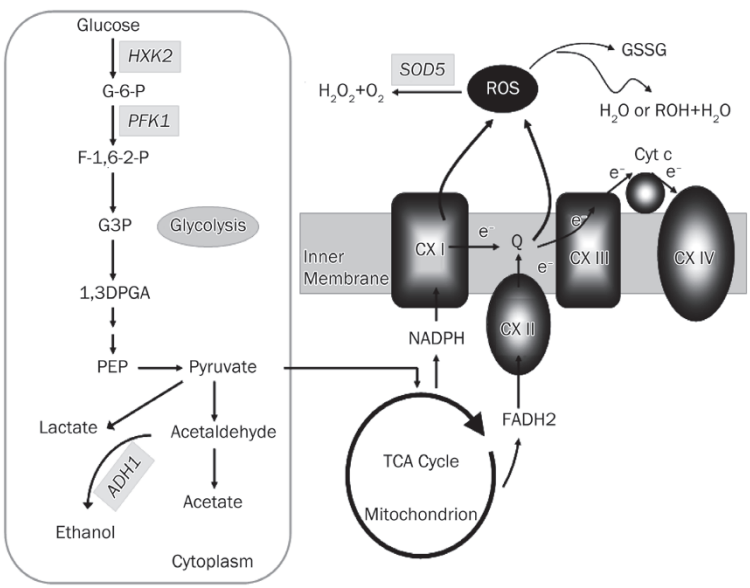

Figure 5. Central carbon metabolism in *C albicans* biofilms during aerobic growth on glucose. The gray ellipses indicate low expression of genes encoded metabolic enzymes participated in aerobic oxidation process after treatment with 10b. The black ellipses indicate augmented tricarboxylic acid cycling process and endogenous reactive oxygen species generation after treatment with 10b. G-6-P, glucose-6-phosphate; F-1,6-2P, fructose-1,6-bisphosphate; G3P, glyceraldehyde-3-phosphate; 1,3-DPGA, 1,3-bisphosphoglycerate; PEP, phosphoenolpyruvate; TCA cycle, tricarboxylic acid cycle.

Table 5. Effect of 10b combined ascorbic acid (AA) on *C albicans* planktonic cells adhesion.

Treatment with PBS	XTT reduction (%)[a] in medium containing 10b and/or ascorbic acid at the concentration of:				
	10b	10b+AA (5 mmol/L)	10b+AA (10 mmol/L)	AA (5 mmol/L)	AA (10 mmol/L)
None wash	51.61±2.41	81.29±4.81[ce]	116.67±8.76[ce]	124.85±8.65	184.94±23.96
Wash twice	92.54±2.82	93.53±2.55	108.46±5.04	118.11±2.80	122.10±10.86

[a] *C albicans* SC5314 planktonic cells containing 10b at 10 μmol/L combined 5, and/or 10 mmol/L ascorbic acid (AA) was incubated for 90 min at 37 °C. XTT reduction is expressed as a percentage of that of control. The results are mean±standard deviations of three independent experiments. Mean±standard error of the mean values (A_{492}) for the controls were 0.226±0.031 without PBS treatment and 0.134±0.019 with PBS washing twice. [c]*P*<0.01 *vs* 10b alone. [e]*P*<0.05 *vs* AA alone.

Table 6. Effect of ascorbic acid (AA) on the inhibition of 10b against *C albicans* biofilm formation and mature biofilm (48 h).

Growth situation	XTT reduction (%)[a] in medium containing 10b and/or ascorbic acid at the concentration of:				
	10b	10b+AA (5 mmol/L)	10b+AA (10 mmol/L)	AA (5 mmol/L)	AA (10 mmol/L)
Biofilm formation [b]	48.35±2.67	52.61±3.28[f]	51.19±4.20[f]	94.33±5.26	103.36±3.24
Mature biofilm (48 h) [c]	72.47±5.04	84.41±4.05[be]	86.22±3.28[be]	101.07±5.90	98.03±2.86

[a] XTT reduction is expressed as a percentage of that of control biofilms. [b] 10b at 10 μmol/L combined 5 and/or 10 mmol/L AA were added to culture of yeasts following the initial 1 h adhesion and incubated for 48 h at 37 °C. [c] 10b at 10 μmol/L combined 5 and/or 10 mmol/L AA were added to mature (48 h) biofilms grown in the absence of the drugs, and incubation was continued for a further 6 h at 37 °C. The results are mean±standard deviations of three independent experiments. [b]*P*<0.05 *vs* 10b alone; [e]*P*<0.05, [f]*P*<0.01 *vs* AA alone.

AA, mature biofilm metabolic activity increased markedly. Our data indicate that ROS augmentation might be a major mechanism of 10b against *C albicans* mature biofilms. This was confirmed by a well known ROS inducer MCZ, which was able to markedly reduce mature biofilm metabolic activity at 10 μmol/L.

Drug binding assays and cell wall component modification studies suggest that cell wall changes may contribute to antifungal biofilm drug resistance[13]. Beta-1,3-glucan is the major structural polysaccharide of the fungal cell wall and is thought to be the main component of the three-dimensional matrix surrounding biofilm cells and closely tied to biofilm formation[47]. In our study, we found that expression of gene *XOG1*, encoding exo-1,3-beta-glucanase enzyme, increased dramatically. This indicated that up-regulated *XOG1* might be another pathway to inhibit biofilm formation because exo-1,3-beta-glucanase enzyme specifically hydrolyzes beta-1,3 glucan, resulting in destruction of the matrix of *C albicans* biofilms and cell wall[48].

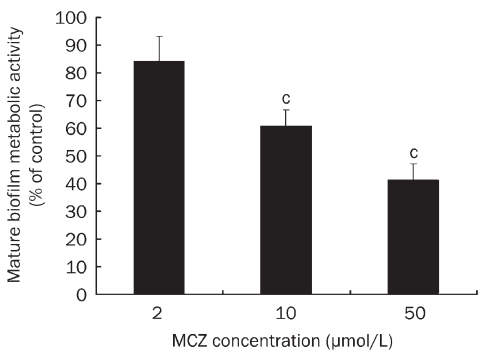

Figure 6. Effect of MCZ incubated for 6 h on mature (48 h) biofilms. MCZ was added to mature (48 h) biofilms and incubation was continued for 6 h at 37 °C. XTT reduction is expressed as a percentage of that of control mature biofilms (48 h) further incubated for 6 h. The results are mean±standard deviations of three independent experiments. Statistically significant differences as determined by Student's *t* test. [b]*P*<0.05, [c]*P*<0.01 *vs* control.

In conclusion, the results of the present study show that 10b treatment altered the expression of biofilm formation-related genes, impaired the ability of *C albicans* to change its morphology, decreased beta-1,3 glucan levels in the biofilm matrix and cell wall, and ultimately blocked *C albicans* to form mature biofilms. In addition, mitochondrial aerobic respiration shift and endogenous ROS augmentation also contributed to reducing mature biofilm metabolic activity. This might provide useful information for the development of new strategies to reduce the incidence of device-associated infections.

Acknowledgements

We thank Dr William A FONZI for kindly offering the isolate *C albicans* SC5314 in this study.

This work was supported by the National Natural Science Foundation of China (30825041, 30500628, and 30630071), National Basic Research Project (2005CB523105), National High Technology Research and Development Program 863 of China (2008AA02Z302).

Author contribution

Yuan-ying JIANG and Yong-bing CAO designed research; Rong-mei LIANG performed the research and wrote the

paper; You-jun ZHOU and Hui TANG synthesized 10b; Yi XU, Ping-hui GAO, Bao-di DAI and Feng YANG critically read the manuscript.

References

1 Ramage G, Saville SP, Wickes BL, Lopez-Ribot JL. Inhibition of *Candida albicans* biofilm formation by farnesol, a quorum-sensing molecule. Appl Environ Microbiol 2002; 68: 5459–63.
2 Sato T, Watanabe T, Mikami T, Matsumoto T. Farnesol, a morphogenetic autoregulatory substance in the dimorphic fungus *Candida albicans*, inhibits hyphae growth through suppression of a mitogen-activated protein kinase cascade. Biol Pharm Bull 2004; 27: 751–2.
3 Nett J, Ande D. *Candida albicans* biofilm development, modeling a host-pathogen interaction. Curr Opin Microbiol 2006; 9: 340–5.
4 Izano EA, Sadovskaya I, Vinogradov E, Mulks MH, Velliyagounder K, Ragunath C. Poly-N-acetylglucosamine mediates biofilm formation and antibiotic resistance in *Actinobacillus pleuropneumoniae*. Microb Pathog 2007; 43: 1–9.
5 Oliveira M, Nunes SF, Carneiro C, Bexiga R, Bernardo F, Vilela CL. Time course of biofilm formation by *Staphylococcus aureus* and *Staphylococcus epidermidis* mastitis isolates. Vet Microbiol 2007; 124: 187–91.
6 Wang C, Li M, Dong D, Wang J, Ren J, Otto M, *et al*. Role of ClpP in biofilm formation and virulence of *Staphylococcus epidermidis*. Microbes Infect 2007; 9: 1376–83.
7 Andes D, Nett J, Oschel P, Albrecht R, Marchillo K, Pitula A. Development and characterization of an *in vivo* central venous catheter *Candida albicans* biofilm model. Infect Immun 2004; 72: 6023–31.
8 Chandra J, Kuhn DM, Mukherjee PK, Hoyer LL, McCormick T, Ghannoum MA. Biofilm formation by the fungal pathogen *Candida albicans*: development, architecture, and drug resistance. J Bacteriol 2001; 183: 5385–94.
9 Baillie GS, Douglas LJ. Matrix polymers of Candida biofilms and their possible role in biofilm resistance to antifungal agents. J Antimicrob Chem 2000; 46: 397–403.
10 Baillie GS, Douglas LJ. Effect of growth rate on resistance of *Candida albicans* biofilms to antifungal agents. Antimicrob Agents Chemother 1998; 42: 1900–5.
11 Baillie GS, Douglas LJ. Iron-limited biofilms of *Candida albicans* and their susceptibility to amphotericin B. Antimicrob Agents Chemother 1998; 42: 2146–9.
12 Nobile1 CJ, Nett JE, Hernday AD, Homann OR, Deneault JS, Nantel A, *et al.* Biofilm matrix regulation by *Candida albicans* Zap1. PLoS Biol 2009; 7: e1000133.
13 Nett J, Lincoln L, Marchillo K, Massey R, Holoyda K, Hoff B, *et al*. Putative role of beta-1,3 glucans in *Candida albicans* biofilm resistance. Antimicrob Agents Chemother 2007; 51: 510–20.
14 Liu H. Transcriptional control of dimorphism in Candida albicans. Curr Opin Microbiol 2001; 4: 728–35.
15 Liu H, Kohler J, Fink GR. Suppression of hyphal formation in *Candida albicans* by mutation of a STE12 homolog. Science 1994; 266: 1723–6.
16 Staab JF, Bradway SD, Fidel PL, Sundstrom P. Adhesive and mammalian Transglut aminase substrate properties of *Candida albicans* Hwp1. Science 1999; 283: 1535–38.
17 Bailey DA, Feldmann PJF, Bovey M, Gow NAR, Brown AJP. The *Candida albicans* HYR1 gene, which is activated in response to hyphal development, belongs to a gene family encoding yeast cell wall proteins. J Bacteriol 1996; 178: 5353–60.
18 Birse CE, Irwin MY, Fonzi WA, Sypherd PS. Cloning and characterization of ECE1, a gene expressed in association with cell elongation of the dimorphic pathogen *Candida albicans*. Infect Immun 1993; 61: 3648–55.
19 Calderone RA, Fonzi WA. Virulence factors of *Candida albicans*. Trends Microbiol 2001; 9: 327–35.
20 Hoyer LL. The ALS gene family of *Candida albicans*. Trends Microbiol 2001; 9: 176–80.
21 Zheng X, Wang YM, Wang Y. Hgc1, a novel hypha–specific G1 cyclin-related protein regulates *Candida albicans* hyphal morphogenesis. EMBO J 2004; 23: 1845–56.
22 Braun BR, Johnson AD. Control of filament formation in *Candida albicans* by the transcriptional repressor TUP1. Science 1997; 277: 105–9.
23 Braun BR, Kadosh D, Johnson AD. NRG1, a repressor of filamentous growth in *Candida albicans*, is down-regulated during filament induction. EMBO J 2001; 20: 4753–61.
24 Li YD, Su C, Mao XM, Cao F, Chen JY. Roles of *Candida albicans* Sfl1 in hyphal development. Eukaryotic Cell 2007; 6: 2112–21.
25 Kadosh D, Johnson AD. Rfg1, a protein related to the *S. cerevisiae* hypoxic regulator Rox1, controls filamentous growth and virulence in *C albicans*. Mol Cell Biol 2001; 21: 2496–505.
26 Kadosh D, Johnson AD. Induction of the *Candida albicans* filamentous growth program by relief of transcriptional repression: a genome-wide analysis. Mol Biol Cell 2005; 16: 2903–12.
27 Nickerson KW, Atkin AL, Hornby JM. Quorum sensing in dimorphic fungi: farnesol and beyond. Appl Environ Microbiol 2006; 72: 3805–13.
28 Hornby JM, Jensen EC, Lisec AD, Tasto JJ, Jahnke B, Shoe-maker R, *et al*. Quorum sensing in the dimorphic fungus *Candida albicans* is mediated by farnesol. Appl Environ Microbiol 2001; 67: 2982–92.
29 Jain N, Kohli R, Cook E, Gialanella P, Chang T, Fries BC. Biofilm formation by and antifungal susceptibility of Candida isolates from urine. Appl Environ Microbiol 2007; 73: 1697–703.
30 Jin Y, Samaranayake LP, Samaranayake Y, Yip HK. Biofilm formation of *Candida albicans* is variably affected by saliva and dietary sugars. Arch Oral Biol 2004; 49: 789–98.
31 Cao YY, Dai BD, Wang Y, Huang S, Xu YG, Cao YB, *et al*. *In vitro* activity of baicalein against *Candida albicans* biofilms. Int J Antimicrob Agents 2008; 32: 73–7.
32 Kohrer K, Domdey H. Preparation of high molecular weight RNA. Methods Enzymol 1991; 194: 398–405.
33 Patterson TA, Lobenhofer EK, Fulmer-Smentek SB, Collins PJ, Chu TM, Bao W, *et al*. Performance comparison of one-color and two-color platforms within the Microarray Quality Control (MAQC) project. Nat Biotech 2006; 24: 1140–50.
34 Eklund AC, Turner LR, Chen P, Jensen RV, Defeo G, Kopf-Sill AR, *et al*. Replacing cRNA targets with cDNA reduces microarray cross-hybridization. Nat Biotechnol 2006; 24: 1071–73.
35 Yang YH, Dudoit S, Luu P, Lin DM, Peng V, Ngai J, *et al*. Normalization for cDNA microarray data: a robust composite method addressing single and multiple slide systematic variation. Nucleic Acids Res 2002; 30: e15.
36 Yao B, Ji HT, Cao YB, Zhou YJ, Zhu J, Lu JG, *et al*. Synthesis and antifungal activities of novel 2-aminotetralin derivatives. J Med Chem 2007; 50: 5293–300.
37 Liang RM, Cao YB, Fan KH, Xu Y, Gao PH, Zhou YJ, *et al*. 2-Aminononyl-6-meth-oxyl-tetralin muriate inhibits sterol C-14 reductase in the ergosterol biosynthetic pathway. Acta Pharmacol Sin 2009; 30: 1709–16.
38 Calderone RA, Fonzi WA. Virulence factors of *Candida albicans*. Trends Microbiol 2001; 9: 327–35.

39 Murad AM, Leng P, Straffon M, Wishart J, Macaskill S, MacCallum DM, *et al*. NRG1 represses yeast-hypha morphogenesis and hypha-specific gene expression in *Candida albicans*. EMBO J 2001; 20: 4742–52.
40 Braun BR, Kadosh D, Johnson AD. NRG1, a repressor of filamentous growth in *Candida albicans*, is down-regulated during filament induction. EMBO J 2001; 20: 4753–61.
41 Moran GP, MacCallum DM, Spiering MJ, Coleman1 DC, Sullivan DJ. Differential regulation of the transcriptional repressor NRG1 accounts for altered host-cell interactions in *Candida albicans* and *Candida dubliniensis*. Mol Microbiol 2007; 66: 915–29.
42 Brookes PS, Darley-Usmar VM. Hypothesis: the mitochondrial NO signaling pathway and the transduction of nitrosative to oxidative cell signals: an alternative function for cytochrome *c* oxidase. Free Radic Biol Med 2002; 32: 370–4.
43 Brookes PS, Levonen AL, Shiva S, Sarti P, Darley-Usmar VM. Mitochondria: regulators of signal transduction by reactive oxygen and nitrogen species. Free Radic Biol Med 2002; 33: 755–64.
44 Kobayashi D, Kondo K, Uehara N, Otokozawa S, Tsuji N, Yagihashi A, *et al*. Endogenous reactive oxygen species is an important mediator of miconazole antifungal effect. Antimicrob Agents Chemother 2002; 46: 3113–7.
45 Kontoyiannis DP. Modulation of fluconazole sensitivity by the interaction of mitochondria and erg3p in *Saccharomyces cerevisiae*. J Antimicrob Chemother 2000; 46: 191–7.
46 Yan L, Zhang JD, Cao YB, Gao PH, Jiang YY. Proteomic analysis reveals a metabolism shift in a laboratory fluconazole-resistant *Candida albicans* strain. J Proteome Res 2007; 6: 2248–56.
47 Nobile1 CJ, Nett JE, Hernday AD, Homann OR, Deneault JS, Nantel A, *et al*. Biofilm matrix regulation by *Candida albicans* zap1. PLoS Biol 2009; 7: e1000133.
48 Humphreys AM, Gooday GW. Properties of chitinase activities from Mucor mucedo: evidence for a membrane-bound zymogenic form. J Gen Microbiol 1984; 130: 1359–66.